Lithium–Ethylamine and Lithium–Sodium–Ethylamine Systems: A Nonmetallic Liquid Electride and the Lowest Melting Fused Salt

Marc G. De Backer,[§] El Bachir Mkadmi,[§] Francois X. Sauvage,[§] Jean-Pierre Lelieur,[§] Michael J. Wagner,[‖] Rosario Concepcion,[‖,†] Judith L. Eglin,[‖,‡] Renee A. Guadagnini,[‖] Jineun Kim,[‖,⊥] Lauren E. H. McMills,[#] and James L. Dye*,[‖]

Contribution from LASIR-HEI-CNRS UPR 2631. 59046 Lille. France. and Department of Chemistry and Center for Fundamental Materials Research. Michigan State University. East Lansing. Michigan 48824

Received January 13. 1994[⊛]

Abstract: Phase equilibria and compound formation in two new alkali metal–amine systems were studied by differential thermal analysis (DTA), EPR, NMR, and magnetic susceptibility methods. Lithium and ethylamine ($EtNH_2$) mixtures with the nominal formula $Li(EtNH_2)_n$ were studied for n = 2–16. A eutectic with $n \approx 5$ melting at T_E = 176.5 ± 0.5 K is present. The presence of an endotherm at T_E from n = 2–16 precludes the existence of solid compounds in this composition range unless they melt with decomposition at the eutectic temperature or decompose at the temperature of a solid–solid transition (T = 124 ± 1 K). EPR line shapes indicate that neither the solid nor the solutions are metallic, and magnetic susceptibilities show that these deep blue-black systems are essentially diamagnetic. Samples that contained equimolar lithium and sodium in ethylamine, which had the nominal formula $LiNa(EtNH_2)_n$, were studied for n = 1–32. Alkali metal NMR studies show that Li^+ and Na^- are present in both the liquid and solid phases. A shiny gold eutectic solution with n = 5–5.5 freezes at 171.3 ± 0.5 K, and a compound with n = 4 melts incongruently at 217.8 ± 0.4 K. There is some evidence for compound formation with n = 2–3.

Introduction

Alkali metals are all very soluble in liquid ammonia.[1,2] Dilute solutions are electrolytic in nature, while concentrated ones become metallic when the mole fraction of metal becomes higher than about 0.04. Only lithium forms a defined compound, which is gold-colored and metallic with the stoichiometry $Li(NH_3)_4$.[3] The solubility of most alkali metals is considerably lower in simple aliphatic amines than in ammonia. However, it has been known for almost a century that lithium and methylamine form a compound, but its composition was not accurately determined.[4,5] It was found later that the compound $Li(CH_3NH_2)_4$ exists and its phase diagram[6,7] and electrical[8,9] and magnetic properties[10,11] have been extensively studied. In the liquid state, it behaves as a rather poorly conducting metal. All other alkali metals are much less soluble in methylamine and give electrolytic solutions that contain alkali cations, with alkali metal anions and/or solvated electrons serving as the counterions.[12] Very little is known about the solubility of lithium in ethylamine except that it is high, but no systematic studies of the properties of concentrated systems have been reported.

The compound $Li(CH_3NH_2)_4$ can be dissolved in solvents in which lithium alone is not soluble (diethyl ether, dimethyl ether, tetrahydrofuran, etc.).[13] It was also reported[13] that $Li(CH_3NH_2)_4$ in methylamine or in other solvents can dissolve equimolar amounts of sodium, and that these lithium–sodium solutions contain sodium in the −1 oxidation state as Na^-, the sodium anion.

It is well-known that salts of the alkali metal anions (alkalides) can be easily obtained in solution in a variety of solvents. Although dilute solutions of alkali metals in ammonia are characterized by the presence of solvated electrons, solutions of sodium in mixtures of ammonia and ethylamine (20:80) show an optical absorption band[14] that can now be assigned to the sodium anion. In general, simple dissolution of alkali metals (except lithium) in amines or in hexamethyl phosphoramide yields solutions that contain alkali metal anions. Metal solubilities are low, however, and the starting metal is recovered upon solvent removal. The solubilization of alkali metals in tetrahydrofuran (THF) and in diethyl ether by the addition of dicyclohexano-18-crown-6 to form alkali metal anions was reported in 1970.[15] This was later extended to other solvents and to other complexants such as cryptands and aza-crown compounds.[16] The proper combination of solvent, alkali metal, and complexant led to the synthesis of a large number of

§ LASIR-HEI-CNRS UPR 2631.
‖ Michigan State University.
† Current address: Department of Natural Sciences, Universidad Pontificia Catolica Madre y Maestra, Santiago, Dominican Republic.
‡ Current address: Department of Chemistry. Mississippi State University. Mississippi State, MS 39762.
⊥ Current address: Department of Chemistry, Gyeongsang National University, Chinju 660-701, Korea.
Current address: Department of Chemistry. Ohio University, Athens, OH 45701.
⊛ Abstract published in *Advance ACS Abstracts*, June 15, 1994.

(1) Das, T. P. In *Advances in Chemical Physics*; Prigogine, I., Ed.; Interscience: New York, 1962; Vol. IV; pp 304–388.
(2) Thompson. J. C. *Electrons in Liquid Ammonia*; Oxford University Press: Oxford, 1976; pp 1–297.
(3) Sienko, M. J. In *Metal–Ammonia Solutions*: Lepoutre, G., Sienko, M. J., Eds.; Benjamin: New York, 1964; pp 25–40.
(4) Moissan, H. *Bull. Soc. Chim. Fr.* **1899**. *21*. 917–21.
(5) Moissan, H. *C. R. Acad. Sci.* **1899**, *128*, 26–30.
(6) Nakamura, Y.; Horie, Y.; Shimoji, M. *J. Chem. Soc., Faraday Trans.* **1974**, *70*, 1376–83.
(7) Hagedorn, R.; Lelieur. J. P. *J. Phys. Chem.* **1980**, *84*, 3652–3654.
(8) Edwards, P. P.; Lusis, A. R.; Sienko. M. J. *J. Chem. Phys.* **1980**, *72*, 3103–3112.
(9) Toma, T.; Nakamura. Y.: Shimoji. M. *Philos. Magn.* **1976**. *33*. 181–187.
(10) Edwards, P. P.; Buntaine, J. R.; Sienko, M. J. *Phys. Rev. B* **1979**, *19*, 5835–5846.
(11) Stacy, A. M.; Johnson, D. C.; Sienko, M. J. *J. Chem. Phys.* **1982**. *76*, 4248–4254.
(12) Dye. J. L. *Prog. Inorg. Chem.* **1984**, *32*, 327–441.
(13) Faber, M. K.; Fussa-Rydel, O.: Skowyra, J. B.; McMills. L. E. H.: Dye. J. L. *J. Am. Chem. Soc.* **1989**, *111*, 5957–5958.
(14) Hohlstein, G.; Wannagat, U. *Z. Anorg. Allg. Chem.* **1957**, *288*, 193–200.
(15) Dye, J. L.; DeBacker, M. G.; Nicely, V. A. *J. Am. Chem. Soc.* **1970**, *92*. 5226–5228.
(16) Dye, J. L.; DeBacker, M. G. *Annu. Rev. Phys. Chem.* **1987**, *38*. 271–301.

0002-7863/94/1516-6570$04.50/0

solid alkalides and electrides.[16-18] These unusual ionic salts are very soluble in a variety of nonreducing organic solvents and they can therefore be used to perform a variety of reductions (concentrations of 10^{-1} M or higher can be obtained in the K-18C6-THF system). Such solutions are especially well suited to carry out reductions that involve the transfer of two electrons.[19] However, the bulk of the alkalide or electride consists of the relatively large macrocyclic complexant, which limits their use in organic synthesis unless the complexant can be easily removed from the reaction mixture.

The simplest solid sodide reported to date[20] has the formula $Li^+(ethylenediamine)_2Na^-$. It is a gold-colored compound that freezes at 250 K but decomposes or decomplexes at 273 K. In this paper we present studies of two other simple systems made of lithium and ethylamine with and without sodium. This system has an advantage over ethylenediamine in that the range of available temperatures at which liquids exist is broader and extends toward lower values, thereby minimizing decomposition problems. All preparations and handling could therefore be carried out at temperatures below 230 K. The phase diagrams of systems that contain equimolar amounts of lithium and sodium metals in the presence of ethylamine, as well as lithium–ethylamine samples without sodium, were determined for a large number of metal concentrations by using differential thermal analysis (DTA). ^7Li and ^{23}Na NMR spectra were obtained to ascertain the nature of the species in solution.

EPR spectroscopy was used to see if transitions to a metallic state occur in lithium–ethylamine solutions. EPR methods have been widely used for the study of the onset of the metallic state in lithium–ammonia and lithium–methylamine solutions. In the former case, the line shape in concentrated liquid solutions could be attributed to the presence of conduction electrons[21] and Dyson's formalism[22] or a modification of it[23] was used for line shape analysis. Similar effects occur at higher concentrations in the lithium–methylamine system.[10,24] The ratio (A/B) of the low- and high-field peak heights of the first derivative EPR spectrum has been frequently used to characterize asymmetric curves, especially when there is evidence for the presence of conduction electrons (CESR).[25] When this ratio is larger than 2.5, as in the case of concentrated Li/NH_3 solutions, the systems can be described in terms of a "dysonian" formalism[22] applicable to thick plates. For lower A/B ratios, another formalism, initially proposed by Webb,[26] has been used for small spherical particles in an inert matrix, where the skin depth d is of the same order as the size a of the particle. Further simplifications have also been used in special cases.[27,28]

Experimental Section

Lithium metal (Fluka or Aldrich) and sodium metal (Merck or Alfa) were handled in a glovebox filled with nitrogen-free dry argon or helium. The mass of the metals could be determined to within 0.1 mg. Prior to making a solution, the metals were dissolved in anhydrous liquid ammonia that was then slowly removed in order to yield the metals in a finely divided state. The metals were then evacuated overnight at room temperature (residual pressure $<10^{-5}$ Torr).

Ethylamine was purified by letting the degassed solvent contact lithium or liquid sodium–potassium alloy until a stable blue solution was obtained at 195 K. After 24 h the ethylamine was distilled under vacuum to storage vessels. The quantities used were determined by either gas volumetric analysis followed by condensation or weighing in small break-seal ampules.

The samples were prepared at low temperature (200 K) by allowing the solvent and the metal to remain in contact for several days. The samples were vigorously shaken at regular intervals and kept at low temperature. Most liquid samples at this temperature are certainly homogeneous, although residual inhomogeneities caused by the formation of solids or solid–liquid mixtures at the highest metal concentrations cannot be completely ruled out.

NMR studies were carried out with a Bruker WH 180 spectrometer. The resonance frequencies of ^7Li and ^{23}Na were 69.95 and 47.62 MHz, respectively. Reported chemical shifts are relative to $Li^+(aq)$ and $Na^+(aq)$ at infinite dilution and were determined by comparison to 0.1 M aqueous solutions of $LiClO_4$ and NaCl. The temperature was regulated by passing the dry N_2 spinning gas through a liquid N_2 heat exchanger and heating it with an in-line heater. Temperature was monitored with a thermocouple placed in the N_2 stream immediately ahead of the entrance to the spinner.

Static susceptibilities were measured with an SHE Corp. Model 800 SQUID susceptometer that can reach temperatures as low as 2 K. The samples were contained in sealed fused silica containers that were suspended in the susceptometer. After the measurements were performed, the samples were allowed to decompose in the cell at room temperature and were run again. This procedure allows subtraction of the diamagnetic susceptibility of the container and the initial sample,[29] even when gaseous decomposition products are formed.

The methods used to prepare samples for EPR work have been previously described.[30] Spectra were recorded on a Bruker ESP 300 spectrometer at X-band. The temperature was controlled by a stream of cold nitrogen regulated to ±1 K.

DTA measurements were performed on a home-built apparatus based on classical designs. It consisted of a brass cylinder (height = 100 mm; diameter = 70 mm) in which two 20-mm wells were drilled symmetrically with respect to the axis of the cylinder. The cell containing the sample was located in one of the wells, while a reference (glass cell filled with aluminum powder) was placed in the other. The cells were made of Pyrex glass having an outside diameter of 16 mm. Containers of this size gave reproducible DTA curves. The amount of solvent was always kept constant at 1.8 g (0.04 mol). The masses of Li and Na metal were adjusted in order to yield the proper concentrations. At the bottom of these cells was an inverted well, 1–2 mm in diameter, into which thermocouples were inserted. These thermocouples were used to measure the sample temperature, with an accuracy of ±0.1 K, and the temperature difference between sample and reference cells, with an accuracy of ±0.01 K. The thermocouples were calibrated with pure compounds that had known melting points. The brass cylinder containing the cells was cooled with liquid nitrogen in a tall narrow Dewar vessel. When the whole system was at liquid nitrogen temperature the cylinder was raised a few centimeters above the liquid nitrogen level and a small regulated dc voltage was applied to a heater wound around the brass block in order to provide a reasonable temperature ramp. Most of the experiments were carried out up to 230 K and each run lasted about 12 h.

DTA curves indicate the transitions that occur in a sample when the temperature is raised. They can detect the presence of solid–solid transitions as well as the melting temperatures of any compounds or solid solutions. Usually the thermograms were recorded starting from the lowest temperature in order to avoid under-cooling phenomena that occur upon slow cooling in the instrument. The shape of the DTA curves is strongly dependent upon the rate of variation of the temperature. Very small heating rates had to be used in order to separate closely spaced peaks.

(17) Dye, J. L.; Ceraso, J. M.; Lok, M. T.; Barnett, B. L.; Tehan, F. J. *J. Am. Chem. Soc.* **1974**, *96*, 608–609.
(18) Tehan, F. J.; Barnett, B. L.; Dye, J. L. *J. Am. Chem. Soc.* **1974**, *96*, 7203–7208.
(19) Jedlinski, Z.; Kowalczuk, M.; Misiolek, A. *J. Chem. Soc., Chem. Commun.* **1988**, 1261–1262.
(20) Concepcion, R.; Dye, J. L. *J. Am. Chem. Soc.* **1987**, *109*, 7203–7204.
(21) Glaunsinger, W. S.; Sienko, M. J. *J. Magn. Reson.* **1973**, *10*, 253–262.
(22) Dyson, F. J. *Phys. Rev.* **1955**, *98*, 349–359.
(23) Damay, P.; Leclerq, F.; Lelieur, J. P. *Philos. Magn. B* **1988**, *57*, 75–91.
(24) Buntaine, J. R.; Sienko, M. J.; Edwards, P. P. *J. Phys. Chem.* **1980**, *84*, 1230–1232.
(25) Edmonds, R. N.; Harrison, M. R.; Edwards, P. P. *Annu. Rep. Prog. Chem. C: Phys. Chem.* **1985**, *82*, 265–308.
(26) Webb, R. H. *Phys. Rev.* **1967**, *158*, 225–233.
(27) Berim, G. O.; Cherkasov, F. G.; Kharakhashyan, E. G.; Talanov, Y. I. *Phys. Status Solidi A* **1977**, *40*, k53–k55.
(28) Guy, S. C.; Edmonds, R. N.; Edwards, P. P. *J. Chem. Soc., Faraday Trans. 2* **1985**, *81*, 937–947.
(29) Landers, J. S.; Dye, J. L.; Stacy, A.; Sienko, M. J. *J. Phys. Chem.* **1981**, *85*, 1096–1099.
(30) De Backer, M. G.; Mkadmi, E. B.; Sauvage, F. X. In *J. Phys. IV Colloque C5, Metals in Solution*; Damay, P., Leclerq, F., Eds.; Les Éditions de Physique: Paris, 1991; Vol. 1, pp 303–308.

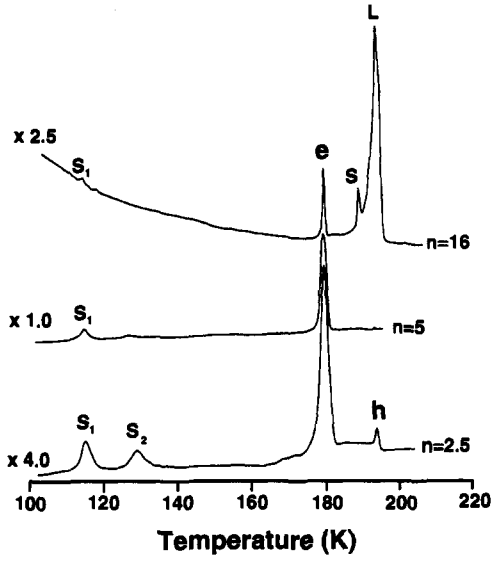

Figure 1. Selected DTA curves of $Li(EtNH_2)_n$: S, S_1, and S_2 are endothermic transitions in the solid, e is the eutectic, L is the liquidus, h is a minor peak observed for small values of n. Both S and h are assigned to pure ethylamine (see text).

Results

Lithium and Sodium in Ammonia. Alkali metal anions have never been observed in liquid ammonia, even in the presence of strong cation complexants such as cryptands. In view of the capability of $Li(CH_3NH_2)_4$ to solubilize large amounts of sodium metal, it was interesting to investigate whether the same was true for $Li(NH_3)_4$. This would be one of the simplest alkalides, having the overall formula $Li^+(NH_3)_n{\cdot}Na^-$. In order to check for its existence, the following experiment was performed: A homogeneous solution of lithium and sodium in liquid ammonia was prepared. Ammonia was then slowly removed until the overall stoichiometry $LiNa(NH_3)_4$ was obtained. The resulting solution was filtered and analyzed for metal content. It was found that essentially only $Li(NH_3)_4$ passed through the filter and that almost no sodium could be detected by emission spectroscopy. We conclude that sodium is not soluble in $Li(NH_3)_4$ and precipitated out upon removal of ammonia; thus, liquid $Li^+(NH_3)_4{\cdot}Na^-$ does not form. This conclusion was checked by an independent method: DTA measurements were performed on a sample having the overall composition $LiNa(NH_3)_8$. After careful thermal annealing of the samples by effecting several temperature cycles, the only peaks remaining were the same as those of a solution of composition $Li(NH_3)_8$; the presence of sodium had no effect.

Lithium–Ethylamine. Thermal effects for *pure* ethylamine are characterized by two transitions. One, at T_s = 184.2 ± 0.5 K, is a solid–solid transition while melting occurs at 191.3 ± 0.5 K. Lithium metal is very soluble in ethylamine, but it forms dark blue solutions that do not have any of the metallic shine seen with concentrated lithium–ammonia and lithium–methylamine solutions. The number of transitions observed in DTA experiments on $Li(EtNH_2)_n$ depended on the concentration of the sample. For $5 \leq n \leq 16$, the DTA curves showed at least three characteristic endothermic peaks. One corresponds to a solid–solid transition (at T_{S_1}), one to the melting of a eutectic (at T_e), and one to the liquidus (at T_L). The solid–solid transition of ethylamine (at T_S) is also present for $n \geq 9$. Above the eutectic concentration, the liquidus peak vanishes. For $n \leq 8$, a new solid–solid peak (at T_{S_2} = 128.5 ± 0.5 K) is observed, as well as a high temperature transition (h), at the melting point of pure ethylamine. Typical DTA curves obtained by warming the sample from liquid nitrogen temperature at a rate of 0.2 to 0.3 deg per min are shown in Figure 1. The transition temperatures observed experimentally for the system $Li(EtNH_2)_n$ are shown as a function of concentration in Figure 2. The solid–solid transition S_1 occurs at 111.8 ± 0.5 K and the eutectic melting temperature T_e is 176.2 ± 0.4 K. Both are concentration independent, whereas the expected temperature dependence is observed for the liquidus curve. The area under the eutectic peak decreases as the metal concentration is lowered, while the area under the liquidus grows under the same conditions. The eutectic concentration corresponds to a value of n between 5 and 5.5. Smaller peaks are occasionally observed, depending on the thermal history of the sample; however, they are only minor features.

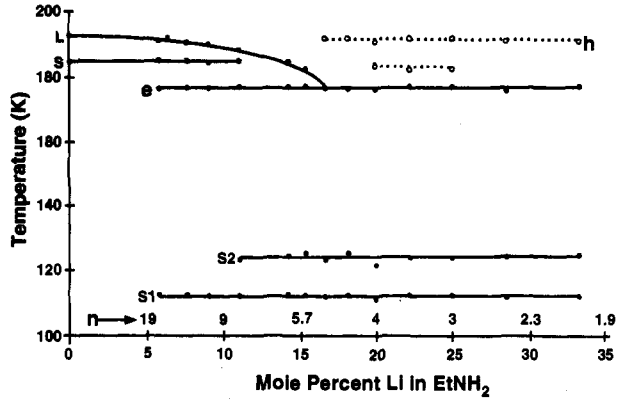

Figure 2. Experimental compositions and temperatures associated with transitions of $Li(EtNH_2)_n$ (open circles correspond to very small DTA peaks).

Magnetic susceptibilities of $Li(EtNH_2)_4$ have been studied down to 2 K. The susceptibility, corrected for the diamagnetic contribution of the constituents (by subtracting the values of the decomposed sample as described above), is diamagnetic. At the lowest temperatures, a "Curie tail" is observed that corresponds to a mole fraction of free spins of less than 10^{-3}. The presence of these unpaired electrons does not markedly affect the bulk susceptibility, but it contributes to the appearance of an EPR signal.

The EPR spectrum of a liquid sample of composition $Li(EtNH_2)_4$ consists of a single line. At high temperature (240 K) it can be fit by a Lorentzian function centered at g = 2.002 with a 3 G line width. As the temperature is decreased, the position remains unchanged but there is a significant broadening of the line toward the "wings" of the peak. The peak shape can then be represented by the sum of two Lorentzian functions centered at the same position. The line width (ΔH_{pp}) of the broader line increases from 4.0 G at 230 K to 6.8 G at 190 K and its relative importance also increases with decreasing temperature. The evolution of the line width of the second peak follows the reverse trend, from 2.6 G at 230 K to 1.5 G at 190 K, while its contribution to the spectrum decreases steadily with decreasing temperature. For temperatures lower than 200 K, there is a very narrow (50 mG) small peak superimposed in the center of the spectrum. The small size of this component as well as uncertainties as to its shape prevented its inclusion in the curve-fitting process.

The EPR spectra of more dilute solutions show only a single line centered at the same position as in the previous case, and of width 0.5 G. Its shape is slightly asymmetric and characterized by an A/B ratio of 1.2. These values remain constant over the whole temperature range. In the solid state, the area under the absorption peak is very small for dilute as well as for concentrated samples. It increases markedly upon melting, and increases further as the temperature is raised above the melting point.

The ^7Li NMR spectra for n = 3 and 5 have chemical shifts that vary from +20 ppm at 200 K to +22 ppm at 225 K to + 25 ppm at 240 K, essentially independent of n in this range. These paramagnetic (Knight) shifts reflect the presence of residual unpaired electron spins in the otherwise diamagnetic sample and probably result from contact density at the lithium nucleus. The

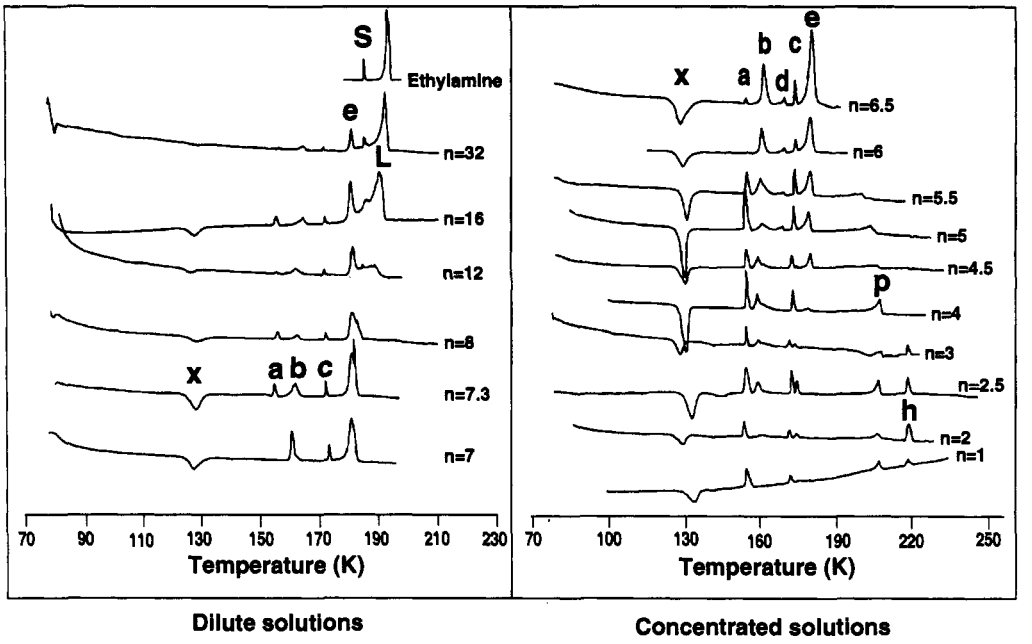

Figure 3. Experimental DTA curves of $Li^+(EtNH_2)_nNa^-$ for various values of n. Note that x is the only exothermic peak.

Table 1. ^7Li and ^{23}Na NMR Chemical Shifts (in ppm) for $Li^+(EtNH_2)_nNa^-$

		chemical shifts			
nucleus	T (K)	$n = 4$	$n = 8$	$n = 12$	$n = 16$
^7Li	253	2.1	2.1	2.9	1.4
	233	2.1	1.7	3.1	1.2
	213	2.0	1.2	2.9	1.6
^{23}Na	253	−58.1	−58.8	−54.7	−58.2
	233	−58.3	−60.1	−54.4	−59.2
	213	−58.5	−60.0	−54.3	−60.1
	193	−59.2		−54.5	−60.2

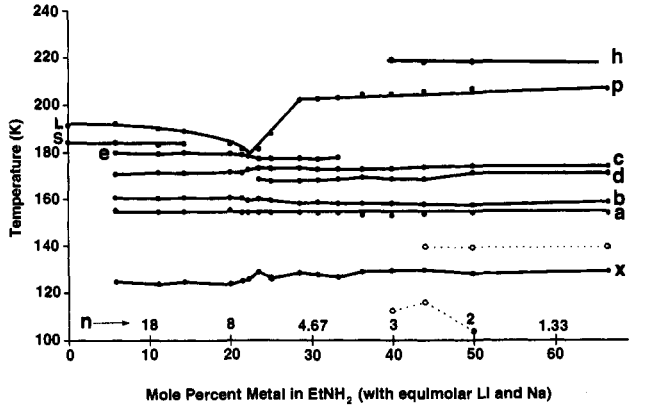

Figure 4. Experimental compositions and temperature associated with transitions of $Li^+(EtNH_2)_x{\cdot}Na^-$ (open circles correspond to very small DTA peaks).

contact density cannot be calculated, however, because of a lack of susceptibility data in this temperature range.

Lithium and Sodium in Ethylamine. Sodium metal is very soluble in these solutions, so that stoichiometries $LiNa(EtNH_2)_n$ can be obtained for n at least as low as 3.0. In contrast to the $Li(EtNH_2)_n$ system, concentrated solutions of $LiNa(EtNH_2)_n$ have a shiny gold color similar to that of concentrated metal ammonia solutions. That sodium is present as Na^- in these systems is demonstrated by alkali metal NMR as well as by their optical reflectance spectra, which show the characteristic peak of Na^- at 600–700 nm.

Solutions of $Li^+(EtNH_2)_n{\cdot}Na^-$ were studied by ^7Li and ^{23}Na NMR spectroscopy in the liquid state for n = 4, 8, 12, and 16. The ^7Li NMR spectra consisted of one symmetric peak with a chemical shift of 2 ± 1 ppm. This peak was both concentration and temperature independent. The ^{23}Na NMR spectra also showed only one symmetrical peak that was also temperature and concentration independent, with a chemical shift of −58 ± 4 ppm. This value is characteristic of Na^- in other compounds and solutions that contain sodium anions.[31,32] The chemical shift data are given in Table 1. The line width (full width at half height) of the ^{23}Na peak was ~100 Hz at temperatures higher than about 200 K. Below that temperature, the system behaved as a frozen sample and the line width increased to ~530 Hz.

Various DTA curves were obtained for this system and were dependent on the composition as defined by n (Figure 3). Only the curves obtained by warming the sample were used. For the more dilute systems ($n > 7$), four peaks were observed in the solid state. An exothermic transition (x) is first observed. It is unique and was not observed for $Li(EtNH_2)_n$. Endothermic peaks labeled a and b are associated with the exothermic peak as described below. All these peaks correspond to processes that occur in the solid state. Annealing at temperatures higher than T_x, T_a, and T_b in separate experiments followed by cooling to liquid nitrogen temperature and repeating the warming process resulted in the disappearance of peaks x, x + a and x + a + b, respectively. Annealing at a temperature higher than T_c resulted in complete recovery of the original signal. The peak labeled e corresponds to the melting of a eutectic at 179.2 ± 0.5 K. It is followed by a liquidus whose temperature depends on the concentration. The concentration of the eutectic corresponds to $n \approx 7.5$. In the more dilute region ($n > 12$), a peak (S) attributed to the solid–solid transition of the pure solvent was observed at 184.2 K.

In the concentration range $n < 7$, a new peak (d) was observed in the solid state at $T_d = 168 \pm 0.4$ K. The position of the "eutectic peak" was slightly shifted (to 177.3 ± 0.2 K) but its area decreased and it disappeared completely for $n = 4$. A concentration-dependent peak (p) appeared above the melting temperature of pure ethylamine that leveled out at 205.5 ± 1.2 K for $n < 4$. In the concentrated region ($n < 4$), the other general features remained unchanged, but one extra peak (h) appeared at 217.8 ± 0.4 K. Figure 4 shows the positions of all the peaks as a function of composition. The most significant temperature values are summarized in Table 2.

(31) Ellaboudy, A.; Tinkham, M. L.; VanEck, B.; Dye, J. L.; Smith, P. B. *J. Phys. Chem.* **1984**, *88*, 3852–3855.
(32) Kim, J.; Dye, J. L. *J. Phys. Chem.* **1990**, *94*, 5399–5402.

Table 2. Average Values of the Temperatures (K) of the DTA Peaks of $Li^+(EtNH_2)_n \cdot Na^-$

composition	T_x	T_a	T_b	T_d	T_c	T_e
$n > 7$	124.4 ± 0.8	154.5 ± 0.5	160.1 ± 0.5		171.3 ± 0.5	179.2 ± 0.5
$4 < n < 7$	127.4 ± 1.2	154.0 ± 0.2	158.7 ± 0.9	167.9 ± 0.4	173.0 ± 0.3	177.3 ± 0.2
$n < 4$	128.8 ± 0.7	153.6 ± 0.7	157.8 ± 0.6	169.6 ± 1.5	173.5 ± 0.6	

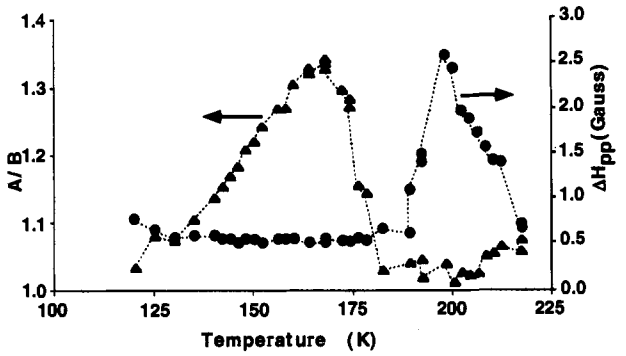

Figure 5. Variation of ΔH_{pp} and of the asymmetry ratio A/B with temperature from the EPR spectra of $Li^+(EtNH_2)_4 \cdot Na^-$.

The bulk magnetic susceptibility of $Li^+(EtNH_2)_4 \cdot Na^-$ was studied down to 2 K. The susceptibility, corrected for the diamagnetic contribution of the constituents, is diamagnetic. At the lowest temperatures a "Curie tail" was observed that corresponds to a mole fraction of unpaired electrons of less than 10^{-3}.

Several samples with concentrations that correspond to $n \approx 4$ and 8 situated on both sides of the eutectic point were studied by EPR spectroscopy. All of these solutions are strong microwave absorbers and it was not possible to get all the sample inside the cavity, even in narrow tubes (1 mm i.d.). Therefore, the spin concentrations could not be evaluated. The variation of the spectra with temperature was studied without changing the sample position. In the frozen state, they were studied at increasing temperatures in order to avoid under-cooling phenomena.

The EPR spectral shapes at low temperatures are strongly dependent upon both temperature and concentration, while, as shown below, their shapes are very similar in the liquid state. The single narrow line ($\Delta H_{pp} \approx 0.6$ G) observed for $Li^+(EtNH_2)_4 \cdot Na^-$ samples below 180 K showed a marked variation of the line shape parameters (Figure 5). At temperatures above 130 K there was significant asymmetry of the line, with A/B increasing to 1.35 at 170 K. Above 170 K, there was a sudden decrease in the asymmetry ratio, followed by an increase in the value of ΔH_{pp} at about 185 K. The concentration of EPR active species, as deduced from double integration of the peaks, increased with temperature, even in the solid state. The spin concentration was about ten times higher at 220 K than below 160 K. The variation of the EPR spectral shape with temperature for $Li^+(EtNH_2)_4 \cdot Na^-$ is shown in Figure 6a.

Samples with the approximate stoichiometry $Li^+(EtNH_2)_8 \cdot Na^-$ had a smaller EPR signal intensity than those with $n \approx 4$. The spectrum observed at low temperatures consisted of a broad peak ($\Delta H_{pp} \approx 20$ G) together with a much narrower peak (Figure 6b). The intensity of the narrow peak, with respect to the broad one, became much more marked as the temperature rose until this peak was the main feature ($\Delta H_{pp} \approx 0.6$ G) at 176 K. The number of spins involved remained constant during this transformation and this narrow peak was asymmetric. When the temperature reached 190 K, the line width suddenly increased ($\Delta H_{pp} \approx 15$ G) and then decreased as the temperature increased. The asymmetry ratio decreased to nearly 1.0. Although these general features were observed for a variety of sample preparations, the relative intensity of the narrow peak with respect to that of the broad peak varied substantially from sample to sample. The overall changes in the spectral shape are shown in Figure 6b. A sample

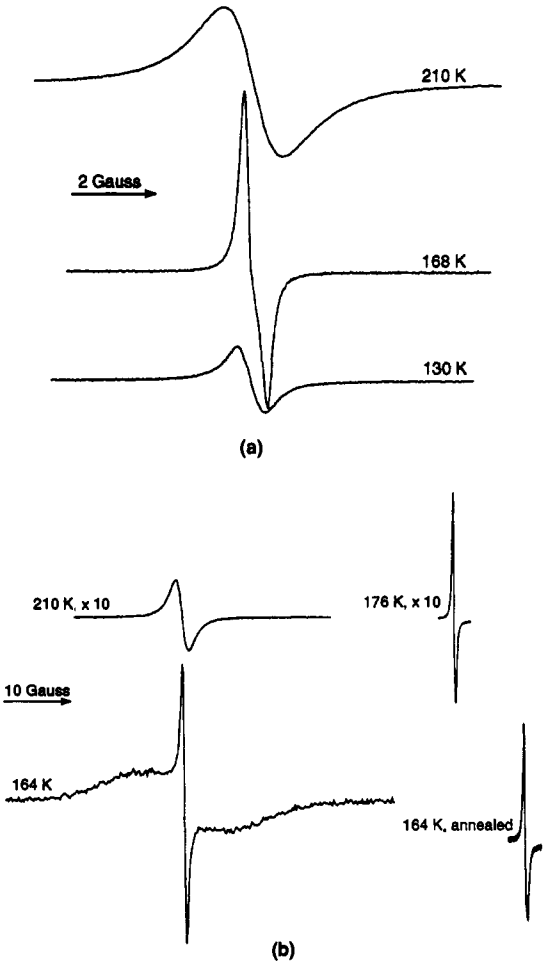

Figure 6. Evolution of the EPR line shape for (a) $Li^+(EtNH_2)_4 \cdot Na^-$ and (b) $Li^+(EtNH_2)_8 \cdot Na^-$ (all curves yield $g = 2.002$).

with this concentration was also studied by lowering the temperature very slowly from the liquid to the solid state. The temperature was lowered a few degrees at a time and allowed to equilibrate before each EPR spectrum was recorded. In the liquid state, the usual broadening of the peak was observed just before reaching the liquidus temperature. At the liquidus temperature, a narrow asymmetric peak ($\Delta H_{pp} = 0.6$ G) appeared, together with the broad peak ($\Delta H_{pp} = 17$ G), and the spectrum was similar to that obtained at low temperatures after rapid cooling. A few degrees below the liquidus, the narrow peak was the main spectral feature and it remained that way down to 100 K. Liquid state spectra consisted of a single, slightly asymmetric line (A/B ratio of the order of 1.05) whose width increased markedly as the temperature was decreased.

Discussion

An important feature of this study is the confirmation of the very high solubility of lithium in ethylamine. Overall mole fractions of metal higher than 0.3 can be easily prepared, but we cannot be certain that such samples are homogeneous. In any event, homogeneous liquid solutions up to 17 mol % of lithium can be prepared. The concentration of the mixed Li–Na system is also extremely high and contrasts with the nearly zero solubility of sodium in ethylamine. These solutions provide the highest

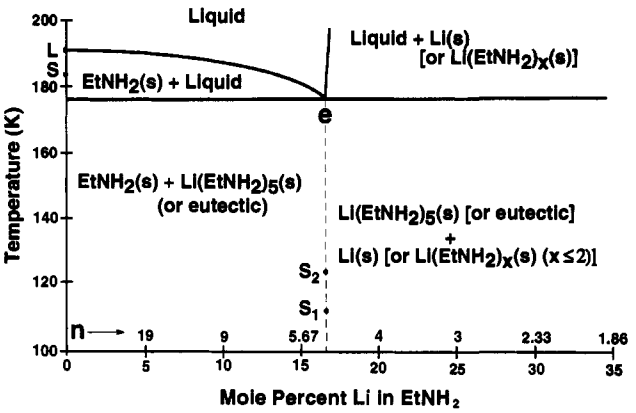

Figure 7. Proposed phase diagram of $Li(EtNH_2)_x$.

Table 3. Area of the Eutectic Peak as a Function of the Number of $EtNH_2$ Molecules per Lithium Atom with a Fixed Quantity of Ethylamine in the Sample

no. ($EtNH_2$/Li)	area (arbitrary units)	no. ($EtNH_2$/Li)	area (arbitrary units)
2.0	26.3	5.5	11.5
2.5	10.0	6.0	13.3
3.0	19.5	8.0	7.0
3.5	11.1	10.0	6.9
4.0	7.8	12.0	4.5
4.5	18.1	16.0	2.5
5.0	17.5		

known liquid concentrations of sodium anions at low temperatures. In fact, the compound $Li^+(EtNH_2)_4{\cdot}Na^-$ could be viewed as the lowest melting fused salt known.

The proposed phase diagram of lithium in ethylamine, which displays the domains of existence of defined compounds, is shown in Figure 7. Only lines corresponding to confirmed equilibrium states are shown. Peaks S_1 and S_2 have small magnitudes compared to that of the eutectic peak, and their relative intensities depend also on the thermal history of the sample. Thus, they are considered to correspond to rearrangements in the solid state and not to equilibrium phase transitions. A puzzling feature in the DTA curves was the appearance of a new high-temperature peak (labeled h in Figure 2) as well as a very small peak at T_S. The temperatures at which these peaks occur are constant and very close to the melting point and solid-state transition temperature of pure ethylamine. From the ratio of the areas of these peaks to those obtained in calibration runs with pure ethylamine, we note that they correspond to the melting of only about 1 mg of ethylamine. It is likely that this amount of ethylamine, which corresponds to only about 0.5% of the quantity of solvent used, may have remained apart from the sample during the cooling process. As a result, these peaks were not used in constructing the phase diagram.

The existence of a defined compound with a unique melting point above the eutectic temperature should result in the disappearance of the eutectic peak at higher metal concentrations. The area of the eutectic peak as a function of n is given in Table 3. A maximum is reached for $n = 5$, as expected from the position of the eutectic. However there is no marked decrease at lower values of n. Indeed, for higher metal concentrations (low n values), the behavior is rather erratic which may reflect the non-homogeneous nature of the more concentrated samples. The continued observation of a substantial eutectic halt implies that either no compound is formed or a compound exists but decomposes at or below the eutectic temperature. The eutectic solution freezes to give an apparently homogeneous blue solid rather than separate phases of Li and $EtNH_2$, which may indicate the formation of a solid solution or the existence of a solid compound, probably either $Li(EtNH_2)_5$ or $Li(EtNH_2)_4$. On the other hand, a colloidal suspension of lithium in solid ethylamine could not be ruled out on the basis of visual observations only.

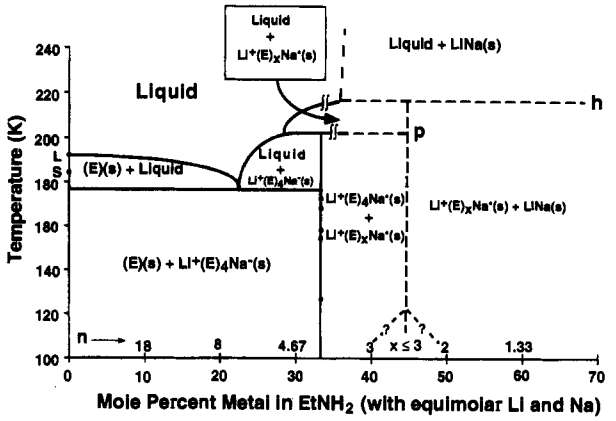

Figure 8. Proposed phase diagram of $Li^+(EtNH_2)_x{\cdot}Na^-$. The non-equilibrium transitions in the solid are represented by solid circles on the $Li^+(EtNH_2)_4{\cdot}Na^-$ line. Information to the right of this compound is highly speculative. The abbreviation E stands for $EtNH_2$.

In order to complete the phase diagram, a nearly vertical saturation line must also be drawn. On the dilute side, solvent peaks can be observed when $n > 8$. This indicates that up to eight solvent molecules are more or less tied up before "free" solvent behavior is encountered. This does not imply a solvation number of eight in dilute solutions, however, since both primary and secondary solvation could be involved.

Static magnetic susceptibility measurements of concentrated $Li(EtNH_2)_x$ systems indicate clearly that most of the electron spins are paired. This is consistent with the observation that in the liquid state the intensity of the EPR signal is small and increases with increasing temperature, indicating that electron pair dissociation occurs. The shapes of the EPR spectra suggest that the major lithium species present in the solid state is not colloidal or precipitated lithium metal. If this were the case, the line width for colloidal lithium would be between 18 and 40 mG, while it would be 300–400 mG for precipitated (bulk) lithium.[33] The observed line width ranges from 1.5 to 6.8 G. It is possible that the small narrow peak that was observed at temperatures below 200 K is due to colloidal lithium, but this is not a major feature. The symmetry of the EPR spectra may also be taken as evidence that the $Li(EtNH_2)_n$ systems are not metallic but can be considered as solid and liquid electrides in which the electrons are largely spin-paired.

The proposed phase diagram of $Li^+(EtNH_2)_n{\cdot}Na^-$ is shown in Figure 8. It indicates clearly that this system is very different from that with lithium alone. The eutectic peak disappears for $n = 4$, demonstrating the presence of a defined compound of stoichiometry $Li^+(EtNH_2)_4{\cdot}Na^-$ with an incongruent melting transition. All transitions observed below the eutectic composition correspond to non-equilibrium states since they can be removed by "annealing". They do not correspond to new solids; therefore, no domains are drawn on the phase diagram. Compounds with $n > 4$ could exist in the solid state, but if they do, they decompose at or below the eutectic temperature.

The high-temperature peak observed for $n \leq 3$ does not correspond to any effect that can be related to solvent melting; it is characteristic of the system. The phase diagram for $n < 4$ relies on the assumption that a new compound corresponding to $2 \leq n \leq 3$ is formed. The possibility that the system is no longer homogeneous for $n < 4$ must also be considered. As previously noted for the Li–$EtNH_2$ system, the nearly vertical line drawn above the second peritectic point corresponds to the saturation curve of the system. The existence of a compound that has fewer than four solvent molecules per lithium cation is known in the

(33) Damay, P.; Sienko, M. J. *Phys. Rev. B* **1976**, *13*, 603–606.

case of $LiNO_3 \cdot 2NH_3$.[34] This ammoniate also has the highest melting temperature among the three existing ones. The coordination about Li^+ is unknown since the crystal structure has not been determined and infrared studies of the vibrations of the NH_3 molecules do not provide any structural clues.[35]

On the dilute side, peaks due to the solid–solid phase transition of the solvent appear for $n \geq 12$. Although this could be an indication of the sum of the solvation numbers of Na^- and Li^+, the suppression of the solid–solid phase transition of $EtNH_2$ by the presence of solvated ions need not correspond to a definite stoichiometry of solvation.

The presence of a non-equilibrium exothermic transition at low temperatures is an interesting feature of this system that is not observed in the LiNa–$MeNH_2$ system.[36] It is always observed over the whole concentration range, whatever the cooling rate, as long as one starts from the molten state. It indicates that the rapid freezing process creates a non-equilibrium state and that, at temperatures of the order of 120 K, the system relaxes to a more stable state, perhaps via rotation of the C_2H_5 group around the N–C bond. The higher temperature endothermic peaks would then correspond to stepwise crystal structure reorganization following this rotation.

Magnetic susceptibility measurements show that the system $Li^+(EtNH_2)_x \cdot Na^-$ is essentially diamagnetic and that there is only a very small concentration of unpaired electrons. This is in agreement with ^7Li and ^{23}Na NMR measurements, which clearly indicate that lithium is present as Li^+ and sodium as Na^-, both ions being diamagnetic. Although these systems have a metallic appearance and contain large relative amounts of both alkali metals, EPR spectroscopy did not indicate the existence of conduction electrons. In the liquid state, the A/B ratio was close to 1.0 and the shape of the signal was Lorentzian. The temperature range of study was limited, however, because above 240 K the signal was lost as one crossed the resonance. This behavior has been previously reported in studies of related systems.[35] Some distorted asymmetric signals were frequently observed in the solid state, but their shape could be due to the presence of anisotropy of the g factor that occurred along with the liquid–solid and/or solid–solid transitions. It should be pointed out that in EPR studies of these systems, one must take great care to ensure that the system is at equilibrium by annealing the samples, to be sure that no metastable states are present. For example, in studies of $Li^+(EtNH_2)_8 \cdot Na^-$, a new broad peak was observed at low temperatures together with the usual narrow peak; the broad peak could be made to disappear by very slow cooling. Care must also be taken to ensure that concentrated liquid solutions are homogeneous, a process that can require several days when one starts with the metals and the solvent. In some cases, fresh samples of $Li^+(EtNH_2)_4 \cdot Na^-$ showed phase separation to a less dense bronze phase and a dark blue phase; however, this behavior was not reproducible and the two phases disappeared with time to yield a single solution phase.

This is the first complete study on the thermal transitions that occur in these low-melting compounds. Except at high metal concentrations, where some refinements may be required concerning the composition of the most concentrated compounds, the diagrams are complete and definite. They provide a map for the study of the behavior of concentrated metal solutions and new alkalide and electride compounds. The study of another, nominally simpler system (Li–Na–CH_3NH_2) will be presented in a separate publication.

Acknowledgment. The French authors thank NATO (Grant No. 0106/88), the Fondation de France, and the Fondation Norbert Segard for financial help at various levels in this study. The U.S. authors also acknowledge the NATO Grant and support from the U.S. National Science Foundation under Solid-State Chemistry Grant No. DMR-90-17292 and from the Michigan State University Center for Fundamental Materials Research.

(34) Portnov, M. A.; Dvilevitch, N. K. *Zh. Obshch. Khim.* **1937**, *7*, 2149–2153.

(35) Regis. A.; Corset, J. *J. Chim. Phys. Phys.-Chim. Biol.* **1972**, *69*, 707–713.

(36) Mkadmi, E. B. Ph.D. Dissertation . Université des Sciences et Technologies de Lille, France, 1993.